

DISCOVERY OF THE UBIQUITOUS CATION NS⁺ IN SPACE CONFIRMED BY LABORATORY SPECTROSCOPY

J. CERNICHAO^{1,2}, B. LEFLOCH³, M. AGÚNDEZ^{1,2}, S. BAILLEUX⁴, L. MARGULÈS⁴, E. ROUEFF⁶, R. BACHILLER⁵, N. MARCELINO^{1,2}, B. TERCERO^{1,5}, C. VASTEL⁷, E. CAUX⁷

(Dated: Received December 14, 2017; accepted January 15, 2018)
Draft version January 18, 2018

ABSTRACT

We report the detection in space of a new molecular species which has been characterized spectroscopically and fully identified from astrophysical data. The observations were carried out with the 30m IRAM telescope^a. The molecule is ubiquitous as its $J=2\rightarrow 1$ transition has been found in cold molecular clouds, prestellar cores, and shocks. However, it is not found in the hot cores of Orion-KL and in the carbon-rich evolved star IRC+10216. Three rotational transitions in perfect harmonic relation $J' = 2/3/5$ have been identified in the prestellar core B1b. The molecule has a $^1\Sigma$ electronic ground state and its $J=2\rightarrow 1$ transition presents the hyperfine structure characteristic of a molecule containing a nucleus with spin 1. A careful analysis of possible carriers shows that the best candidate is NS⁺. The derived rotational constant agrees within 0.3-0.7% with ab initio calculations. NS⁺ was also produced in the laboratory to unambiguously validate the astrophysical assignment. The observed rotational frequencies and determined molecular constants confirm the discovery of the nitrogen sulfide cation in space.

The chemistry of NS⁺ and related nitrogen-bearing species has been analyzed by means of a time-dependent gas phase model. The model reproduces well the observed NS/NS⁺ abundance ratio, in the range 30-50, and indicates that NS⁺ is formed by reactions of the neutral atoms N and S with the cations SH⁺ and NH⁺, respectively.

Keywords: ISM: clouds — line: identification — molecular data — radio lines: ISM

1. INTRODUCTION

In molecular clouds nitrogen is mainly in the form of N₂, which is unobservable directly via its rotational spectrum. Diazenylium (N₂H⁺) is usually used as a tracer of N₂ (Daniel et al. 2006, 2007, 2013). Major N-bearing molecules in the gas phase of interstellar clouds are HCN, HNC, CN, NH₃, ammonium (NH₄⁺), the protonated ion of NH₃ (see Cernicharo et al. 2013, and references therein), and NCCN/NCCNH⁺ (Agúndez et al. 2015). Many other N-bearing species, such as the radicals C_nN and the cyanopolyynes, have been studied in detail and their chemistry is rather well understood (see Agúndez & Wakelam 2013, and references therein). However, only three N-bearing species containing sulfur have been detected so far: NS, HNCS, and HSCN. Nitrogen sulfide (NS) was detected in the early years of radioastronomy by Gottlieb et al. (1975) and it has been observed in practically all interstellar environments, even in comets (Irvine et al. 2000). Although a recent study of the chemistry of sulfur in cold dense clouds has been carried out by Fuente et al. (2016), the formation pathways of these molecules are far from well understood. The gas-phase chemistry of cold dark clouds is mainly

based on the reactions between ions and neutrals (Agúndez & Wakelam 2013). However, only a small percentage ($\approx 15\%$) of the detected species are ions (cations or anions). The last diatomic cation identified in space is NO⁺, which was detected towards B1b with an abundance ratio NO/NO⁺ ~ 500 (Cernicharo et al. 2014), similar to the abundance ratio SO/SO⁺ (~ 1000) observed in the same source by Fuente et al. (2016).

In this Letter we report on the discovery for the first time in space of the nitrogen sulfide cation, NS⁺. This species has been fully characterized through three rotational transitions, one of them exhibiting hyperfine structure due to the presence of nitrogen, and its detection in space has been confirmed by laboratory spectroscopy.

2. OBSERVATIONS

The observations presented in this paper are part of a complete spectral line survey at 3, 2, and 1 mm of a set of interstellar clouds harboring different physical conditions within the IRAM large program ASAI⁸ (Lefloch et al. 2017). They have been complemented in this work with data at 3 mm of B1b and TMC1 (Marcelino et al. 2005, 2007, 2009; Marcelino 2007; Cernicharo et al. 2012, 2013) and various dark clouds observed in a search for molecular anions (Agúndez et al. 2015b).

All observations were performed between 2006 and 2017 with the IRAM 30m radiotelescope, located at Pico Veleta (Spain), using different sets of receivers and spectrometers (see references above). System temperatures were in the range 80-300 K. Pointing errors were always within 3". Spectra were calibrated in antenna temperature corrected for atmospheric attenuation using the ATM package (Cernicharo 1985; Pardo et al. 2001). All data were processed using the GILDAS

¹ Group of Molecular Astrophysics. ICMM. CSIC. C/ Sor Juana Inés de La Cruz 3, E-28049, Madrid, Spain

² Dpt. of Molecular Astrophysics. IFF. CSIC. C/ Serrano 123, E-28006, Madrid, Spain

³ Université Grenoble Alpes, CNRS, IPAG, 38000 Grenoble, France

⁴ Laboratoire de Physique des Lasers, Atomes et Molécules, UMR 8523 CNRS, Université Lille, 59655 Villeneuve d'Ascq Cedex, France.

⁵ Observatorio Astronómico Nacional (OAN, IGN), Calle Alfonso XII, 3, 28014 Madrid, Spain

⁶ LERMA, Observatoire de Paris, PSL Research University, CNRS, Sorbonne Universités, UPMC Univ. Paris 06, F-92190 Meudon, France

⁷ IRAP, Université de Toulouse, CNRS, UPS, CNES, Toulouse, France

^a This work was based on observations carried out with the IRAM 30-meter telescope. IRAM is supported by INSU/CNRS (France), MPG (Germany) and IGN (Spain).

⁸ <http://www.oan.es/asai>

software package⁹.

3. RESULTS

In all observed sources, a line at 100198.55 ± 0.08 MHz emerges as one of the strongest unidentified features. The frequency uncertainty includes a source velocity error of 0.15 km s^{-1} . Figure 1 shows the observed spectra in TMC1, B1b, and L483, and clearly suggests the presence of hyperfine structure of a low- J transition, most likely the $J = 2 \rightarrow 1$ transition of a molecule containing a nucleus with spin 1. Two additional lines at frequencies $3/2$ (150295.611 ± 0.08 MHz) and $5/2$ (250481.477 ± 0.08 MHz) have been found in B1b (see Figure 1 bottom panels). They correspond to the $J = 3 \rightarrow 2$ and $5 \rightarrow 4$ transitions of a new molecular species. None of these lines can be identified using the catalogues CDMS (Müller et al. 2005) and JPL (Pickett et al. 1998). The possible candidates are discussed in next section.

The three unidentified lines, including the hyperfine structure of the $J = 2 \rightarrow 1$ one, have been fitted to the standard Hamiltonian of a linear molecule including nuclear quadrupolar coupling providing $B = 25049.919 \pm 0.010$ MHz, $D = 35.42 \pm 0.20$ kHz, and $eQq = -5.93 \pm 0.10$ MHz (for a nuclear spin of 1).

The $J = 2 \rightarrow 1$ line has been detected towards all cold sources that we have examined, but also in shocks, and in the warm envelopes of SgrB2 and the hot corino IRAS4A in which the kinetic temperature is ≈ 30 K (see Figure 2). However, it is not detected towards the hot cores of Orion KL (data from Tercero et al. 2010), SgrB2(N) (public data from Belloche et al. 2013) and the carbon-rich star IRC+10216. Physical parameters for the sources are given in Table 1.

3.1. Astrophysical identification of NS^+

We have checked that $2/3/5$ harmonic relation found in B1b cannot correspond to higher values of the rotational quantum number by searching for lines that could be present if B was half or a third of the measured value (i.e., harmonic relations $4/6/10$ or $6/9/15$). We conclude that this harmonic relation is the only possible one characterizing spectroscopically the three observed lines. We have also checked that the lines are not associated to any other nearby feature of similar intensity (± 1 GHz) that could indicate a doublet electronic state. We conclude that the molecule is linear with a $^1\Sigma$ electronic ground state.

Being a close-shell molecule with $B \sim 25.05$ GHz, the number of candidates is not very large. The species has to include only H, N, C, O or S (silicon- or metal-bearing species are not detected in cold dark clouds). Moreover, the molecule has to be diatomic, or triatomic containing H, in order to have this relatively large rotational constant. Furthermore, the molecule has to contain N as it is the only nucleus with spin 1. Hence, our carrier is NX or HXN/HNX ($X=C,S,O$), neutral or cation. Anions are unlikely because negative ions have not been detected in most of the observed sources. HCN and HNC have a much larger rotational constant. The same applies to HNO. The best candidates could be HCS, HSC, HNS, HSN (neutral or cations). HCS and HSC are well studied in the laboratory, are slightly asymmetric, have doublet electronic ground states and their $(B+C)/2$ values are around 20 GHz. Their cations could have a slightly larger rotational constant but for HCS⁺ $B \sim 21.4$ GHz (Margules et al. 2003).

No laboratory data are available for HSC⁺. *Ab initio* calculations by Puzzarini (2005) indicated that it is bent with $(B+C)/2$ too low. HSN and HNS are both bent with singlet and triplet ground electronic states, respectively (Yaghlane et al. 2014). Their cations are also bent with doublet ground electronic states and too low $(B+C)/2$ (Yaghlane et al. 2014; Trabelsi et al. 2016). Hence, no reasonable triatomic species can be found as carrier of our lines.

If the carrier is a diatomic species it must contain sulfur or phosphorus in order to have the correct order of magnitude for the rotational constant. None of the well known diatomic species (CS, SO, PS, PO, PN, NS, CP) fit the observed B . All their cations, except NS^+ and PO^+ , have spin multiplicity >1 in their ground electronic state. For example, CS^+ , has a $^2\Sigma^+$ electronic state, $B = 25.9$ GHz and $D = 41.3$ kHz (Baillieux et al. 2008), while CP^+ has a $^3\Pi$ ground electronic state with $B_e \sim 21.5$ GHz (Bruna & Peyerimhoff 1980). PO^+ has a singlet electronic state with $B = 23.512$ GHz (Petrmichl et al. 1991). Hence, the only remaining plausible candidate is NS^+ .

Several *ab initio* calculations have been performed for NS^+ (Dyke et al. 1977; Karna & Grein 1986; Peterson & Woods 1988; Yaghlane et al. 2005; Yaghlane & Hochlaf 2009). All of them predict a $^1\Sigma^+$ ground electronic state. From the photoelectron spectrum of NS, $r_e(\text{NS}^+)$ was estimated to be 1.440 ± 0.005 Å (Dyke et al. 1977). The calculated values for α_e , the vibrational contribution to the rotational constant, range (in MHz) between 120 (Yaghlane & Hochlaf 2009) and 180 (Peterson & Woods 1988). These estimations provide an equilibrium rotational constant 24.9-25.2 GHz and B_0 between 24.84 and 25.11 GHz. The agreement with our rotational constant, 25.05 GHz, is within 0.3-0.7%. The estimated distortion constant by Peterson & Woods (1988), 36 kHz, is also in excellent agreement with the value we have derived from our lines (35.4 kHz). Moreover, Peterson & Woods (1988) computed the quadrupole coupling constant, eQq , to be -6.54 MHz, which compares very well with our value of -5.95 MHz. Consequently, the excellent agreement between our rotational constants and the *ab initio* calculations strongly support NS^+ as the carrier of our lines which has been finally confirmed in the laboratory (see section 3.3).

3.2. Column densities

B1b is the only source where we have more than one NS^+ line and thus we can study its excitation conditions. The calculated *ab initio* dipole moment of NS^+ is 2.17 D (Peterson & Woods 1988), a value which requires a large density to pump efficiently the $J=5$ rotational level. No collisional rates are available for NS^+ . The molecule is isoelectronic to CS and thus we have adopted the collisional rates for CS calculated by Lique & Spielfiedel (2007) scaled up by a factor 5 to take into account that NS^+ is an ion (see, e.g., the case of HCO^+ and CO).

The molecule has been implemented into the MADEX code (Cernicharo 2012) which provides standard LTE or LVG calculations based on the formalism of Goldreich & Kwan (1974). For densities $n(\text{H}_2) > 10^6 \text{ cm}^{-3}$ the rotational levels up to $J = 5$ could be nearly thermalized. For typical values of $n(\text{H}_2)$ in cold dense cores of a few 10^5 cm^{-3} , $T_k = 10-15$ K, the rotational temperature of the $J = 2 \rightarrow 1$ line will be just 2-3 K below T_k . However, for lower densities the $J = 2 \rightarrow 1$ transition could be subthermally excited. Hence, we have estimated the column density of NS^+ using the LVG approximation for

⁹ <http://www.iram.fr/IRAMFR/GILDAS/>

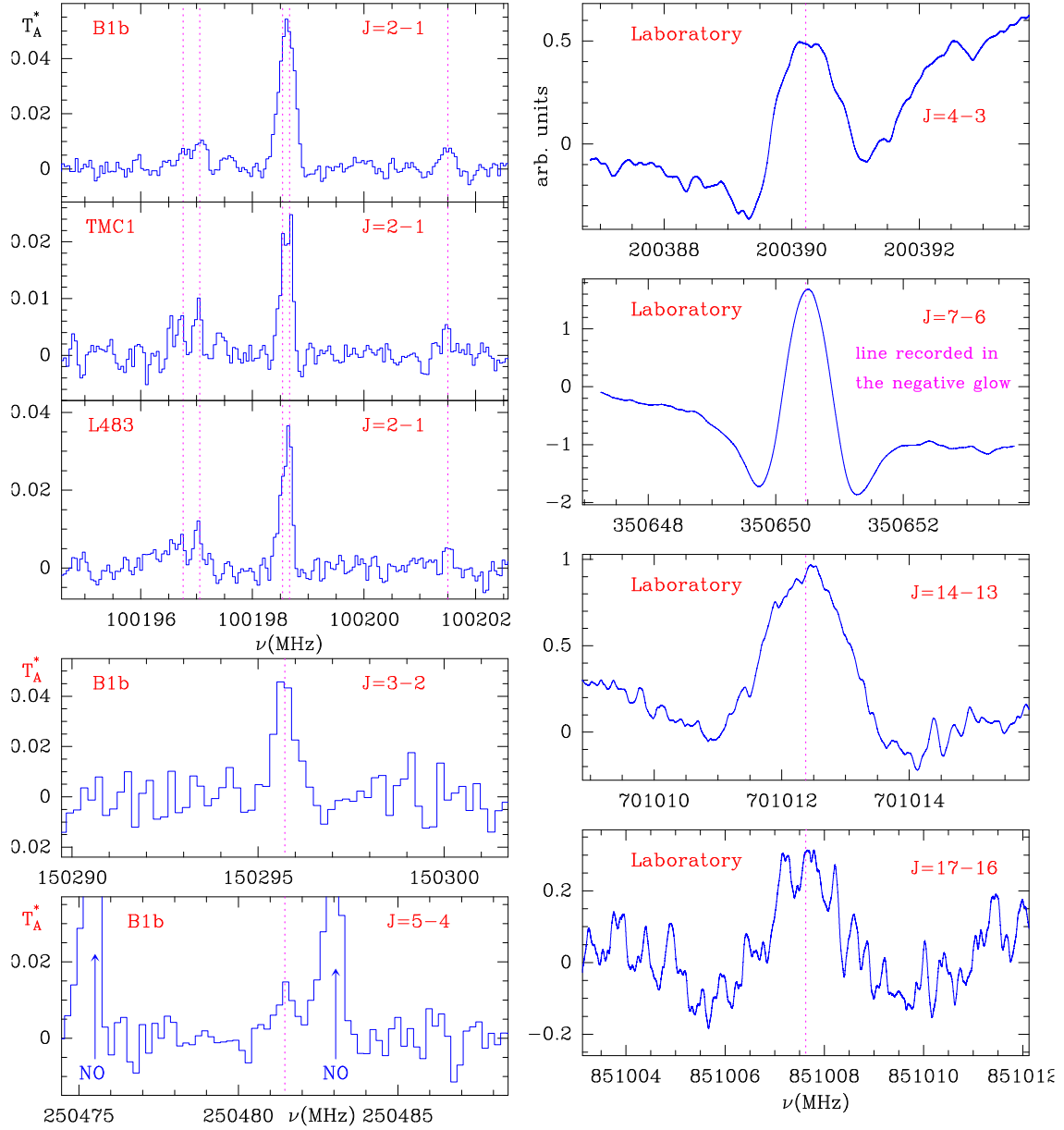


Figure 1. **Left upper panels:** Observed feature at 100198.55 MHz in B1b, TMC1, and L483. Vertical dashed lines indicate the position of the hyperfine component calculated from the fit to this line and those shown in the bottom panels. The hyperfine structure is computed for a nuclear spin of 1. **Left bottom panels:** Observed lines in B1b corresponding to the $J=3\rightarrow 2$ ($\nu_0=150295.611\pm 0.080$ MHz) and $J=5\rightarrow 4$ ($\nu_0=250481.477\pm 0.080$ MHz) transitions of NS⁺. Vertical dashed lines indicate the position of the calculated frequencies. **Right panels:** Some laboratory transitions recorded in the positive column discharge (except otherwise mentioned) in Ar, CS₂ and atmospheric air.

all observed clouds. Although the collisional rates are very uncertain our calculations indicate that the $J=2-1$ line is close to thermalization for the physical conditions given in Table 1.

The three lines observed towards B1b, assuming that B1b fills the beam at the three observed frequencies, can be fitted with $n(\text{H}_2) = 10^5 \text{ cm}^{-3}$, $T_k = 12 \text{ K}$ (Marcelino et al. 2007; Cernicharo et al. 2012), and $N(\text{NS}^+) = 2 \times 10^{11} \text{ cm}^{-2}$. The beam averaged total gas column density towards B1b could be a few 10^{22} cm^{-2} (Cernicharo et al. 2012), and thus the fractional abundance of NS⁺ in B1b is a few 10^{-12} relative to H₂.

We have derived column densities of NS in the sources for which data is available assuming LTE because no collisional rates are available for this species. For TMC1, L1544

and the cold envelope of SgrB2 only data on the $J=5/2\rightarrow 3/2$ are available. However, for B1b, IRAS4a, L1157mm, and L1157B1 several transitions have been observed (from $J=5/2\rightarrow 3/2$ up to $11/2\rightarrow 9/2$). No NS data was available for the other sources. LTE could underestimate the column density because the excitation temperature of the high J lines will be subthermal. In order to evaluate the extent of non-LTE excitation we have adopted the collisional rates of CS for NS and computed its excitation conditions neglecting its fine and hyperfine structure. The excitation temperature obtained for the unsplitted lines was assumed to be the same for all fine and hyperfine components. For the physical conditions of the clouds, the LVG method results in NS column densities 1.5-2.5 times larger than assuming LTE. Hence, the final NS col-

Table 1
Source parameters and derived column densities for NS⁺ and NS

| Source | α_{2000} (h:m:s) | δ_{2000} ($^{\circ}$ ' '') | V_{LSR} (km s ⁻¹) | Δv^a (km s ⁻¹) | T_A^{*b} (mK) | $n(\text{H}_2)$ (cm ⁻³) $\times 10^5$ | $N(\text{H}_2)$ (cm ⁻²) $\times 10^{22}$ | T_k (K) | $N(\text{NS}^+)$ (cm ⁻²) $\times 10^{10}$ | $N(\text{NS})$ (cm ⁻²) $\times 10^{12}$ | R^c | Ref. |
|-----------------------------|----------------------------|---------------------------------------|------------------------------------|---------------------------------------|--------------------|---|--|--------------|---|---|-------------|------|
| IRAS4A | 03:29:10.42 | 31:13:32.2 | 7.4 | 1.19 | 17.0 | 20.0 | 37.0 | 30 | 22.6 | 10.0 | 44 | 1 |
| B1b | 03:33:20.80 | 31:07:34.0 | 6.5 | 0.97 | 54.5 | 1.0 | 15.0 | 12 | 20.0 | 10.0 | 50 | 2 |
| L1495B | 04:15:41.80 | 28:47:46.0 | 7.7 | 0.42 | 12.6 | 0.1 | 1.2 | 10 | 4.0 | ... | ... | 3 |
| L1521F | 04:28:39.80 | 26:51:35.0 | 6.4 | 0.38 | 13.7 | 11.0 | 14.0 | 10 | 1.7 | ... | ... | 3 |
| TMC1 | 04:41:41.88 | 25:41:27.0 | 5.7 | 0.69 | 23.8 | 0.5 | 1.0 | 10 | 5.2 | 1.7 | 33 | 2 |
| L1544 | 05:04:17.21 | 25:10:42.8 | 6.9 | 0.59 | 11.4 | 0.8 | 9.4 | 12 | 2.3 | 1.2 | 52 | 4 |
| Lupus-1A | 15:42:52.40 | -34:07:53.5 | 5.0 | 0.47 | 15.8 | 5.0 | 1.5 | 14 | 4.2 | ... | ... | 3 |
| L483 | 18:17:29.80 | -04:39:38.0 | 5.3 | 0.70 | 36.7 | 0.4 | 3.0 | 10 | 8.5 | ... | ... | 3 |
| Serpens South 1a | 18:29:57.90 | -01:56:19.0 | 7.4 | 1.03 | 23.0 | 0.1 | 2.0 | 11 | 8.5 | ... | ... | 3 |
| L1157-mm | 20:39:06.30 | 68:02:15.8 | 2.6 | 1.20 | 12.0 | 0.6 | 0.6 | 12 | 9.1 | 2.6 | 29 | 5 |
| L1157-B1 | 20:39:10.20 | 68:01:10.5 | 2.6 | 2.95 | 8.0 | 5.0 | 0.1 | 60 | 40.0 | 13.0 | 33 | 5 |
| Orion KL (HC ^d) | 05:35:14.50 | -05:22:30.0 | 5.0 | ... | ... | 500.0 | 42.0 | 225 | ≤ 100 | 3000 | ≥ 3000 | 6 |
| Orion KL (CR ^e) | 05:35:14.30 | -05:22:37.0 | 7.5 | ... | ... | 10.0 | 7.5 | 110 | ≤ 100 | 500 | ≥ 500 | 6 |
| SgrB2 (envelope) | 17:47:43.00 | -28:23:12.1 | 66.0 | 10.0 | 35.0 | 0.1 | ... | 30 | 100 | 50 | 50 | 7 |

^{a,b} Observed Δv and T_A^* for the $J = 2 \rightarrow 1$ main component of NS⁺.

^c R is the NS/NS⁺ abundance ratio.

^{d,e} The hot core and compact ridge components of the cloud.

References for adopted densities and temperatures: (1) Lefloch et al. (1998); (2) Cernicharo et al. (2012, 2013); Fuente et al. (2016); Marcelino et al. (2007); (3) Agúndez et al. (2015b); Loison et al. (2016); (4) Quénard et al. (2017); (5) Lefloch et al. (2012); (6) Tercero et al. (2010); (7) Tercero et al., in preparation.

umn densities are uncertain within a factor 2.

The derived column densities of NS⁺ (assuming $E(J = 2) = 5.01340 \text{ cm}^{-1}$) and NS are given in Table 1. The NS/NS⁺ abundance ratio ranges between 30 and 50. In B1b this abundance ratio is 50, which is ~ 10 and ~ 20 times smaller than the abundance ratios NO/NO⁺ (Cernicharo et al. 2014) and SO/SO⁺ (Fuente et al. 2016), respectively.

3.3. Laboratory detection

To corroborate the astrophysical discovery, we set up an experiment to detect NS⁺ by rotational spectroscopy below 1 THz. The salient features of the spectrometer have been thoroughly described in Bermudez et al. (2017). Briefly, millimeterwave radiation was obtained by the frequency multiplication of an E8257D synthesizer referenced to a GPS-locked Rubidium atomic clock. The instrumental resolution of the frequency multiplier chain is better than 1 Hz at 1 THz and the achievable resolution is typically 500 kHz at 0.5 THz. The cation was produced in a Pyrex absorption cell by glow discharging a mixture of N₂ and CS₂ (Merck). H₂S (purity: 99.9999%) and OCS could also be used as sources of sulfur. A solenoid coil wound on the cell could be used to magnetically extend the negative glow region.

We first examined the chemistry by assessing the $J = 9.5 \leftarrow 8.5$ transition (e parity) at 438050.1 MHz of the NS radical ($^2\Pi_{1/2}$) in a positive column discharge. Compared to H₂S, CS₂ was more efficient and hold stable discharge conditions. Contrary to expectation, NO yielded a S/N enhancement of 2-3 over N₂ and atmospheric air instead of NO further increased the S/N by a factor 2.

The astronomical line at 250481.477 MHz was then inspected. It was readily detected with optimum conditions analogous to those used for producing NS, i.e. CS₂ and atmospheric air were preferable: P(argon) = P(air) = 7.5 mTorr, P(CS₂) = 3.5 mTorr. We have afterwards measured the transition frequencies between 150 – 850 GHz, corresponding to $J' = 3 - 17$. Our error measurement is better than 50 kHz except for the line measured near 851 GHz (≈ 120 kHz).

Table 2
Laboratory transition frequencies (in MHz) of NS⁺ below 1 THz

| $J' \leftarrow J''$ | ν_{obs} | Δv^a | $J' \leftarrow J''$ | ν_{obs} | Δv^a |
|---------------------|-------------------------|--------------------|---------------------|--------------------------|--------------------|
| 3 \leftarrow 2 | 150295.607 | 0.002 | 12 \leftarrow 11 | 600955.245 | -0.004 |
| 4 \leftarrow 3 | 200390.216 | 0.003 | 13 \leftarrow 12 | 650989.258 | -0.021 |
| 5 \leftarrow 4 | 250481.463 | 0.007 | 14 \leftarrow 13 | 701012.396 | 0.025 |
| 6 \leftarrow 5 | 300568.504 | 0.011 | 15 \leftarrow 14 | 751023.687 ^b | 0.013 ^c |
| 7 \leftarrow 6 | 350650.500 | 0.019 | 16 \leftarrow 15 | 801022.380 ^b | 0.016 ^c |
| 8 \leftarrow 7 | 400726.582 | 0.003 | 17 \leftarrow 16 | 851007.624 | 0.013 |
| 9 \leftarrow 8 | 450795.933 | -0.014 | 18 \leftarrow 17 | 900978.540 ^b | 0.027 ^c |
| 10 \leftarrow 9 | 500857.724 | -0.018 | 19 \leftarrow 18 | 950934.324 ^b | 0.033 ^c |
| 11 \leftarrow 10 | 550911.123 ^b | 0.006 ^c | 20 \leftarrow 19 | 1000874.121 ^b | 0.040 ^c |

^a $\Delta v = \nu_{obs} - \nu_{calc}$.

^b Predicted transition.

^c Uncertainty is given instead of Δv .

Derived molecular constants: $B_0 = 25049.89843(50)$ MHz, $D_0 = 35.0567(17)$ kHz, $H_0 = 0$ (fixed value); $\sigma = 14$ kHz.

All lines were recorded in a positive column discharge, using $V_{dc} = 1.4$ kV and $I_{dc} = 50$ mA (ballast resistor ≈ 10 k Ω). To prove that the carrier is a cation, the discharge conditions were switched to a magnetically confined negative glow discharge, applying $V_{dc} = 4.2$ kV and $I_{dc} = 20$ mA (ballast resistor ≈ 100 k Ω). Indeed, it is known that the negative glow (a nearly electric field-free region) is the region that produces a far higher concentration of cations (compared to the positive column), and it is a common technique to lengthen the negative glow by applying a longitudinal magnetic field (De Lucia et al. 1983), as this region is usually very short (a few cm). Enhancements in signal strength (up to two orders of magnitude) with this approach are expected for close-shell cations only.

The $J = 7 \leftarrow 6$ transition was monitored while increasing the intensity of the magnetic field. The line, very weak without magnetic field, was about 5 times as strong, compared to the positive column discharge conditions, for a magnetic field of about 200 G. The measured frequency of this transition was identical (within 5 kHz) in both discharge conditions, showing

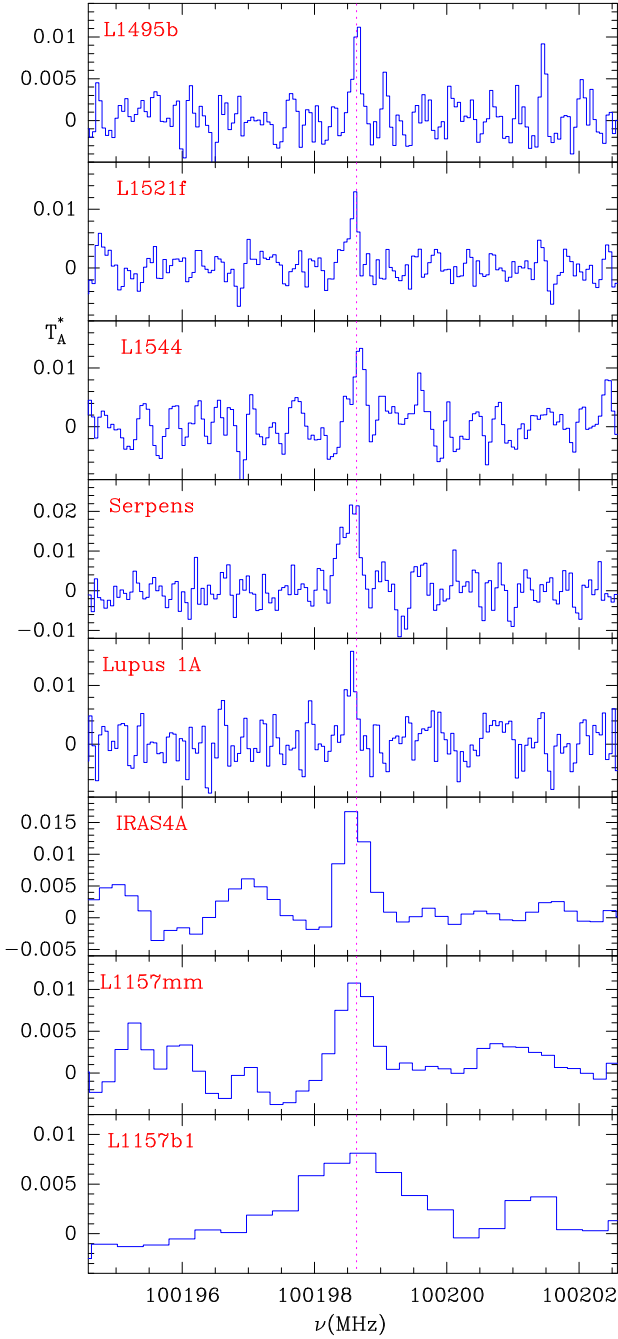


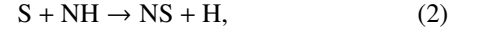
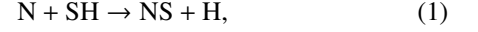
Figure 2. Observed $J=2\rightarrow 1$ transition of NS⁺ towards different sources.

that in the positive column lines are unshifted by the Doppler effect. This is as expected given the mass of the cation. Only lightest ions such as SH⁻ (Civis et al. 1998), OD⁻ and N₂H⁺ (Cazzoli & Puzzarini 2005) have their frequency Doppler-shifted in the microwave region.

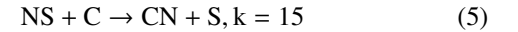
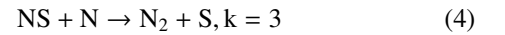
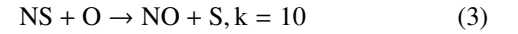
Various laboratory lines are shown in Figure 1 and Table 2 provides laboratory frequencies and the derived rotational and distortion constants. The agreement with the astrophysical and *ab initio* constants is excellent. Since the cation contains nitrogen and sulfur we conclude that the only possible carrier is NS⁺. The observed S/N was too weak to observe N³⁴S⁺ in natural abundance.

4. DISCUSSION

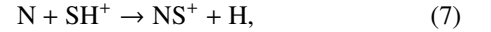
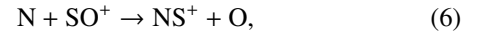
The chemistry of NS and NS⁺ in dense interstellar clouds has been poorly investigated so far (e.g., Agúndez & Wakelam 2013). The chemistry of sulfur in molecular clouds has been recently revisited by Fuente et al. (2016) and Vidal et al. (2017), although unfortunately no prediction was provided for the abundances of NS or NS⁺ in these studies. Here we consider the chemistry of dense clouds, with special attention to NS and NS⁺. Nitrogen sulfide (NS) is assumed to be formed through the neutral-neutral reactions



for which the adopted rate constants are $10^{-10} \text{ cm}^3 \text{ s}^{-1}$ (KIDA database; Wakelam et al. 2015), while it is mostly destroyed through reactions with neutral atoms (rates in units of $10^{-11} \text{ cm}^3 \text{ s}^{-1}$ from KIDA database)



The resulting modeled abundance of NS is thus very dependent on the assumed elemental abundances of N, O, S, and on the C/O elemental ratio. The NS⁺ ion, on the other hand, is principally formed through reactions of atomic nitrogen with the SO⁺ and SH⁺ molecular ions



The rate coefficient of reaction (6) is of the order of $5 \times 10^{-11} \text{ cm}^3 \text{ s}^{-1}$, according to a flowing afterglow measurement by Fehsenfeld & Ferguson (1973). No experimental information is available for reaction (7), which is estimated to be $7.4 \times 10^{-10} \text{ cm}^3 \text{ s}^{-1}$ in the KIDA database. NS⁺ is principally destroyed through dissociative recombination with electrons and reactions with neutral atoms (O, N, and C). No measurement nor theoretical estimate is yet available for the dissociative recombination (*DR*) of NS⁺ and a conservative value of $2 \times 10^{-7} (T/300)^{-0.5} \text{ cm}^3 \text{ s}^{-1}$ is given in the KIDA database, thought to be representative for *DR* of diatomic ions. It is worth noting that observations show a rather uniform NS/NS⁺ column density ratio across the observed sources (see Table 2) which is not directly linked to any formation scenario of NS⁺ from NS. Indeed, the charge exchange reaction of NS with H⁺ and C⁺, although thought to be rapid, will not be an efficient source of NS⁺ in dense clouds where atomic ions are very rare.

We display in Figure 3 gas-phase time-dependent model results for NS and NS⁺ as well as for NO, NO⁺, SO, and SO⁺ for dense cloud conditions typical of B1b (Cernicharo et al. 2012). The chemical network is built from that used in Roueff et al. (2015) where the coupling between N and S chemistries involving NS, NS⁺, HNS⁺ has been introduced, following the reactions available in the KIDA database. C, N, and S are assumed to be depleted to account for adsorption on grains: C/H = 7×10^{-6} , N/H = 1×10^{-6} , S/H = 8×10^{-8} , and C/O = 0.7. The fractional abundances of NS, NS⁺, SO⁺ and NO⁺ ions in B1b are shown to be reasonably reproduced whereas the SO and NO neutral radicals are somewhat underproduced and overproduced, respectively, in the model. More experimental and theoretical efforts are obviously needed to better constrain the chemistry of NS and NS⁺ in molecular clouds.

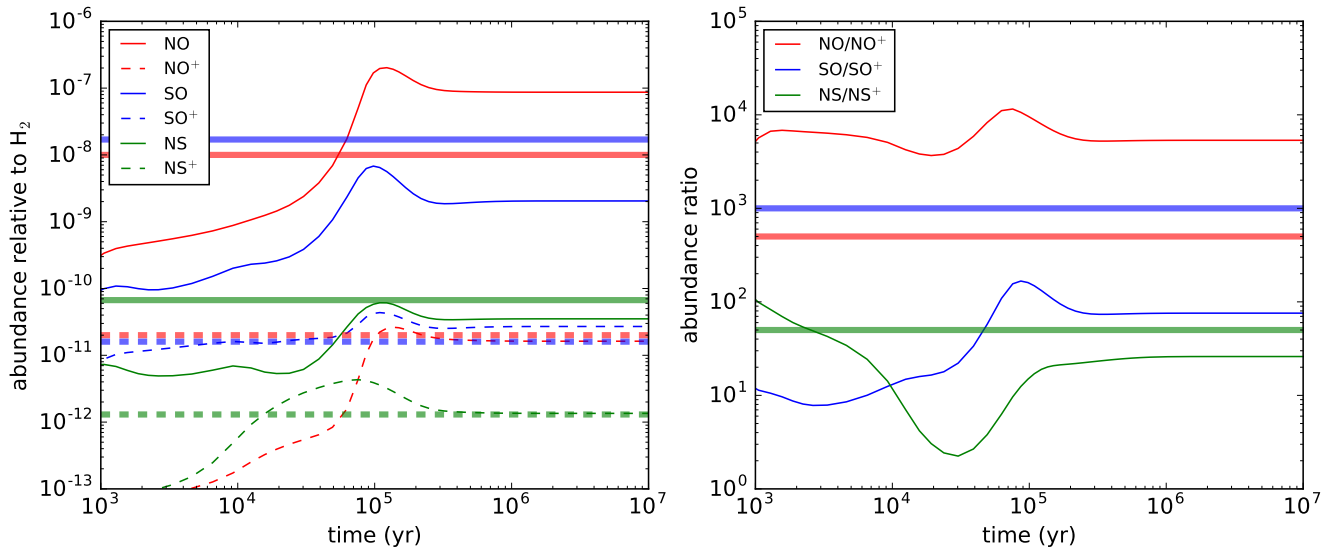


Figure 3. Calculated abundances of NO, NO⁺, SO, SO⁺, NS, and NS⁺ relative to n(H₂) as a function of time for n(H₂)=10⁵ cm⁻³ and T = 12K (left) and the corresponding ratios NO/NO⁺, SO/SO⁺, and NS/NS⁺ (right). The observed values in B1b are indicated by horizontal thick lines.

A large NS/NS⁺ ratio, as observed in hot cores, is the signature of a different formation mechanism of NS⁺ which is rather coming from charge exchange reactions of relatively abundant NS with C⁺ and H⁺. Although the fraction of sulfur locked by NS⁺ in the observed sources is relatively low (10 ppm at most), the fact that this ion is ubiquitous in dark clouds of different evolutionary stages makes it a good potential tracer of the physical and chemical conditions of such environments.

We thank funding support from Spanish MINECO (grants AYA2012-32032, AYA2016-75066-C2-1-P, CSD2009-00038, and RyC-2014-16277) and from European research Council (grant ERC-2013-SyG 610256, NANOCOSMOS). This work was also supported by the Programme National PCMI CEA and CNES, and the French National Research Agency (ANR-13-BS05-0008-02 "IMOLABS").

REFERENCES

- Agúndez, M. & Wakelam, V. 2013, *Chem. Rev.*, 113, 8710
 Agúndez, M., Cernicharo, J., de Vicente, P., et al., *A&A*, 579, L10
 Agúndez, M., Cernicharo, J., & Guélin, M. 2015, *A&A*, 577, L5
 Bailleux, S., Walters, A., Grigorova, E., Margulès, L., 2008, *ApJ*, 679, 920
 Belloche, A., Müller, H. S. P., Menten, K. M., et al., 2013, *A&A*, 559, A47
 Bermudez, C., Bailleux, S., Cernicharo, J., 2017, *A&A*, 598, A9
 Bruna, P.J., Peyerimhoff, S.D., 1980, *J. Chem. Phys.*, 72, 5437
 Cazzoli, G., Puzzarini, C., 2005, *J. Chem. Phys.*, 123, 041101
 Cernicharo, J., 1985, Internal IRAM report (Granada: IRAM)
 Cernicharo, J., 2012, in *ECLA-2011: Proc. of the European Conference on Laboratory Astrophysics*, EAS Publications Series, 2012, Editors: C. Stehl, C. Joblin, & L. d'Hendecourt (Cambridge: Cambridge Univ. Press), 251 (http://www.icmm.csic.es/nanocosmos/?page_id=1619)
 Cernicharo, J., Marcelino, N., Roueff, E., et al., 2012, *ApJ*, 759, L43
 Cernicharo, J., Tercero, B., Fuente, A., et al., 2013, *ApJ*, 771, L10
 Cernicharo, J., Bailleux, S., Alekseev, E., et al., 2014, *ApJ*, 795, 40
 Civis, S., Walters, A., Tret'yakov, M. Y., et al., 1998, *J. Chem. Phys.*, 108, 8369
 Daniel, F., Cernicharo, J., & Dubernet, M.L., 2006, *ApJ*, 648, 461
 Daniel, F., Cernicharo, J., Roueff, E., et al., 2007, *ApJ*, 667, 980
 Daniel, F., Gerin, M., Roueff, E., et al., 2013, *A&A*, 560, A3
 De Lucia, F. C., Herbst, E., Plummer, G. M., 1983, *J. Chem. Phys.*, 78, 2312
 Dyke, J.M., Morris, A., & Trickle, I.R., 1977 *J. Chem. Soc. Faraday Trans. 2*, 73, 147
 Fehsenfeld, F. C. & Ferguson, E. E. 1973, *J. Geophys. Res.*, 78, 1699
 Fuente, A., Cernicharo, J., Roueff, E., et al., 2016, *A&A*, 593, A94
 Goldreich, P., Kwan, J., 1974, *ApJ*, 189, 441
 Gottlieb, C., Ball, J.A., Gottlieb, E.W., et al., 1975, *ApJ*, 193, L89
 Irvine, W.M., Senay, M., Lovell, A.J., et al., 2000, *Icarus*, 143, 412
 Kama, S.P., Grein, F., 1986, *Chem. Phys.*, 109, 35
 Lefloch, B., Castets, A., Cernicharo, J., et al., 1998, *A&A*, 334, 269
 Lefloch, B., Cabrit, S., Busquet, G., 2012, *ApJ*, 757, L25
 Lefloch, B., Ceccarelli, C., Codella, C., et al., 2017, *MNRAS*, 469, L73
 Lique, F., Spielfiedel, A., 2007, *A&A*, 462, 1179
 Loison, J.-C., Agúndez, M., Marcelino, N., et al. 2016, *MNRAS*, 456, 4101
 Marcelino, N., Cernicharo, J., Roueff, E., et al., 2005, *ApJ*, 620, 308
 Marcelino, N., 2007, PhD Thesis, Univ. Granada, Spain.
 Marcelino, N., Cernicharo, J., Agúndez, M., et al., 2007, *ApJ*, 665, L127
 Marcelino, N., Cernicharo, J., Tercero B., Roueff, E., 2009, *ApJ*, 690, L27
 Margules, L., Lewen, F., Winnewisser, et al., 2003, *Phys. Chem. Chem. Phys.*, 5, 2770
 Müller, H.S.P., Schlöder, F., Stutzki, J., Winnewisser, G., 2005, *J. Mol. Struct.*, 742, 215
 Pardo, J. R., Cernicharo, J., Serabyn, E. 2001, *IEEE Trans. Antennas and Propagation*, 49, 12
 Petrmichl, R.H., Peterson, K.A., Woods, R.C., 1991, *J. Chem. Phys.*, 94, 3504
 Peterson, K.A., Woods, R.C., 1988, *J. Chem. Phys.*, 89, 4929
 Pickett, H.M., Poynter, R.L., Cohen, E.A., et al., 1998, *J. Quant. Spectrosc. Radiat. Transfer*, 60, 883
 Puzzarini, C., 2005, *J. Chem. Phys.*, 123, 024313
 Quénard, D., Vastel, C., Ceccarelli, C., et al., 2017, *MNRAS*, 470, 3194
 Roueff, E., Loison J.-C., Hickson K., 2015, *A&A*, 576, A99
 Tercero, B., Cernicharo, J., Pardo, J.R., Goicoechea, J., 2010, *A&A*, 517, A96
 Trabelsi, T., Yaghlane, S.B., Al Mogren, M.M., et al., 2016, *J. Chem. Phys.*, 145, 084307
 Vidal, T. H. G., Loison, J.-C., Yassin Jaziri, A., et al. 2017, *MNRAS*, 469, 435
 Wakelam, V., Loison, J.-C., Herbst, E., et al. 2015, *ApJS*, 217, 20
 Yaghlane, S.B., Lahmar, S., Lakhdar, Z. B., Hochlaf, M., 2005, *J. Phys. B: At. Mol. Opt. Phys.*, 38, 15101
 Yaghlane, S.B., Hochlaf, M., 2009, *J. Phys. B: At. Mol. Opt. Phys.*, 42, 15101
 Yaghlane, S.B., Jaidane, N.E., Cotton, C.E., et al., 2014, *J. Chem. Phys.*, 140, 244309